

## INTERACTION BETWEEN Lu CATIONS AND 2:1 ALUMINOSILICATES UNDER HYDROTHERMAL TREATMENT

MARÍA D. ALBA\* AND PABLO CHAIN

Instituto Ciencia de los Materiales de Sevilla, Departamento de Química Inorgánica, CSIC, Universidad de Sevilla, Avenida Américo Vespucio, s/n 41092 Seville, Spain

**Abstract**—Smectites are considered to be an important component in backfill barriers due to their marked swelling and high cation exchange capacity. Both properties are affected considerably when these clays transform under natural conditions. However, we have recently described a chemical interaction between high-activity radionuclide simulators and smectites which could prove to be effective at immobilizing radionuclides definitively. Investigating the efficiency of this mechanism, independent of bentonite ageing, is a challenge. For this purpose, the reactivity shown by a non-expandable layered aluminosilicate, muscovite, has been compared to that shown by an expandable one, beidellite. Both samples were treated hydrothermally with a solution of lutetium nitrate, and the transformations were studied by X-ray diffraction, nuclear magnetic resonance and scanning electron microscopy/energy dispersive X-ray analysis. Lutetium cations react with the silicon framework of both 2:1 layered aluminosilicates under hydrothermal conditions, and new phases, lutetium disilicate, kaolinite, boehmite and natrosilite are generated. The results demonstrate that the efficiency of the chemical mechanism is not determined by the swelling and the cation exchange capacity of 2:1 layered aluminosilicates. Thus, the rare earth disilicate formation might account for the success of the clay barrier, once bentonite has lost its swelling and cation exchange capacity.

**Key Words**—Bentonite, CEC, Hydrothermal Alteration, Lutetium Cations, Nuclear Waste Barriers, Radionuclide Barriers.

### INTRODUCTION

Deep geological repositories are considered in the scientific community to be the most promising sites for disposing of nuclear waste containing long-lived radionuclides. In a future repository, one of the ways that radionuclides may return to the Earth's surface and the biosphere is by groundwater-induced dissolution of the canister and the glass, and by subsequent transport by deep waters. In order to protect canisters from water intrusion and to eventually trap the radioelement released, waste-forms will be isolated from the surrounding geological media by several barriers. There are diverse opinions regarding the geological features of appropriate locations for disposal sites. However, disposal strategies for all nations assume that waste isolation will be maintained by reliance on a combination of engineered and natural barriers between the emplaced waste and the environment. Moreover, all countries have evolved towards using more robust engineered barrier systems to compensate for the uncertainties in the performance of natural barriers. Among them, the engineered backfill barrier will be essentially composed of clays.

Smectites, 2:1 layered silicates with layer charges ranging from 0.4 to 1.2 (Bailey, 1980) are considered to be an important component in backfill barriers due to their

dual properties: a marked swelling and a high cation exchange capacity (CEC). Swelling will limit the access by water to the waste packages and, accordingly, reduce corrosion. A high CEC helps to retain radioactive nuclides, once they have escaped from the metal container. Any change in either of the two clay properties will influence the operation of the backfill barrier (Tsunashima *et al.*, 1981; Borovec, 1981; Ames *et al.*, 1982, 1983; Miller *et al.*, 1982; Morris *et al.*, 1994; Oades, 1984; Dent *et al.*, 1992; Heimann, 1993; Yamada and Nakazawa, 1993; Chisholm-Brause *et al.*, 1994). It is well known that under natural conditions, the swelling ability and CEC of smectite can change (Jennings and Thompson, 1986; Eberl *et al.*, 1993; Cuadros and Linares, 1996). Moreover, Bauer *et al.* (2001) observed that the reaction of the radioactive fluids with clays results in a decrease in CEC and reduced adsorption of positively charged radionuclide species onto the smectitic materials would be expected. This is, therefore, considered to be a key problem for its use as a barrier for waste disposal (Meunier *et al.*, 1998; Bauer *et al.*, 2001).

On the other hand, we have recently observed that when a smectite sample is in contact with an aqueous solution of a lanthanide salt (simulating radionuclide) at pressures and temperatures close to those expected in deep geological disposal, a chemical reaction occurs leading to the formation of an insoluble lanthanide disilicate phase (Alba *et al.*, 2001). Although this mechanism might be effective at immobilizing the highly active radionuclide, it is important to investigate

\* E-mail address of corresponding author:

alba@icmse.csic.es

DOI: 10.1346/CCMN.2005.0530105

the efficiency of this mechanism independently of bentonite longevity, *i.e.* independently of the swelling and cation exchange properties of the clays.

Thus, it is the aim of this paper to compare the behavior of a non-expandable layer silicate with that of an expandable one under hydrothermal conditions in a lanthanide aqueous solution. The formation of the insoluble disilicate phase from the non-expandable silicate would indicate that the loss of CEC and swelling properties by bentonite may not be a serious problem for its use in the engineered barrier. However, the existence of similar chemical interactions between bentonite and those long-lived radioactive wastes that are not simulated by rare earth cations should be tested, in order to evaluate the engineering barrier safety. For this purpose, we have selected two phyllosilicate samples: a non-expandable mica and an expandable smectite. The main differences in the samples are in the CEC and swelling ability.

## EXPERIMENTAL METHODS

### Material

**Starting materials.** Beidellite, SBCa-1, (structural formula:  $\text{Na}_{0.67}^{\text{IV}}(\text{Si}_{7.56}\text{Al}_{0.44})^{\text{VI}}(\text{Al}_{3.63}\text{Mg}_{0.19}\text{Fe}_{0.18})\text{O}_{20}(\text{OH})_4$  plus 5% of kaolinite) (Becerro, 1997) was obtained from the the Source Clays Repository of The Clay Minerals Society, formerly located at the University of Missouri (Columbia), while the muscovite used (Pérez-Maqueda *et al.*, 2003) (structural formula:  $\text{K}_{2.0}^{\text{IV}}(\text{Si}_{6.0}\text{Al}_{2.0})^{\text{VI}}(\text{Al}_{3.72}\text{Mg}_{0.08}\text{Fe}_{0.15}\text{Ti}_{0.06})\text{O}_{20}(\text{OH})_4$ ) came from Sierra Albarrana, (Córdoba, Spain).

**Hydrothermal treatments.** The powdered samples were suspended in 50 mL of  $\text{Lu}(\text{NO}_3)_3$  solution, in a molar ratio of  $\text{Lu}/\text{Si} = 1.1$  and were heated at 300°C for 3 days in a stainless steel reactor (Perdigón, 2002). The reaction products were collected by filtering, washed with distilled water and dried in air at 60°C. Although it is well known that geochemical processes of waste degradation and waste/rock interaction in the hydrothermal environment remain predictable to temperatures up to ~200°C (Mather *et al.*, 1982; Savage and Chapman, 1982; Allen and Wood, 1988), many studies devoted to simulating deep geological disposal conditions use temperatures of up to 350°C to increase reaction rates (Mather *et al.*, 1982; Savage and Chapman, 1982; Allen and Wood, 1988).

### Experimental techniques

**X-ray powder diffraction (XRD).** Diffraction patterns were obtained using a diffractometer (Kristalloflex D-500 Siemens) at 40 kV and 40 mA with Ni-filtered  $\text{CuK}\alpha$  radiation and a graphite monochromator. Samples were prepared using a side-packed aluminum holder. The XRD patterns were recorded over the range 3 to 70°2 $\theta$  at a step size of 0.05° and with a counting time of 10 s per step. The background was subtracted from raw intensity data inter-

actively using the computer program "X'Pert HighScore" (produced by Philips Analytical B.V. Almelo, The Netherlands. © Koninklijke Electronics N.V.).

**Scanning electron microscopy (SEM).** The morphology and chemical composition of the samples were analyzed using a scanning electron microscope (JEOL JSM 5400) equipped with a LINK Pentafet probe and ATW windows for energy dispersive X-ray (EDX) analysis.

**Nuclear magnetic resonance (NMR) measurements.** Single-pulse spectra were recorded using a Bruker DRX400 spectrometer equipped with a multinuclear probe using a magnetic field of 9.36 T. Powdered samples were packed in 4 mm zirconia rotors and spun at 12 kHz. The  $^{29}\text{Si}$  MAS (magic angle spinning) NMR spectra were acquired at a frequency of 79.49 MHz, using a  $\pi/6$  pulse width of 2.7  $\mu\text{s}$  and a pulse space of 3 s. The  $^{27}\text{Al}$  MAS-NMR spectra were recorded at 104.26 MHz with a  $\pi/20$  pulse width of 1.6  $\mu\text{s}$  and delay time of 3 s. The chemical shifts are reported in ppm from tetramethylsilane for  $^{29}\text{Si}$  and from 0.1 M solutions of  $\text{AlCl}_3$  for  $^{27}\text{Al}$ .

## RESULTS AND DISCUSSION

### Muscovite

Figure 1a shows the XRD patterns of the untreated muscovite; it reveals numerous basal reflections and the *hkl* reflections which are compatible with the  $2M_1$  polytype and with a perfect ordering of the layers with respect to each other. After the hydrothermal treatment, the XRD pattern (Figure 1b) shows several new reflections in addition to the muscovite reflections and they are consistent with the development of two new crystalline phases,  $\text{Lu}_2\text{Si}_2\text{O}_7$  (JCPDS file number 35-0326) and boehmite (JCPDS file number 76-1871). The residual mica structure indicates that complete dissolution and replacement of the muscovite with new phases did not occur, but instead, muscovite was gradually replaced by the new phases.

The SEM image of the mica submitted to hydrothermal treatment (Figure 2a) shows three different types of particles. The irregular rough particles show EDX lines (Figure 2b) corresponding to the  $\text{K}\alpha_1$  and  $\text{M}\alpha_1$  lines of Si and Lu, respectively, and they are the main constituents of  $\text{Lu}_2\text{Si}_2\text{O}_7$ . Other particles were composed of large flakes and had an EDX spectrum (Figure 2c) with  $\text{K}\alpha_1$  lines of Si, Al and K, which are the main constituents of muscovite. These data are in agreement with the XRD results and indicate that the hydrothermal treatment at 300°C did not considerably alter the layer morphology of the starting mica, the lamellar structure of which is seen clearly in the micrograph. Finally, an EDX spectrum of small particles was observed (Figure 2d) with mostly  $\text{K}\alpha_1$  lines of Al from boehmite which was also identified by XRD.

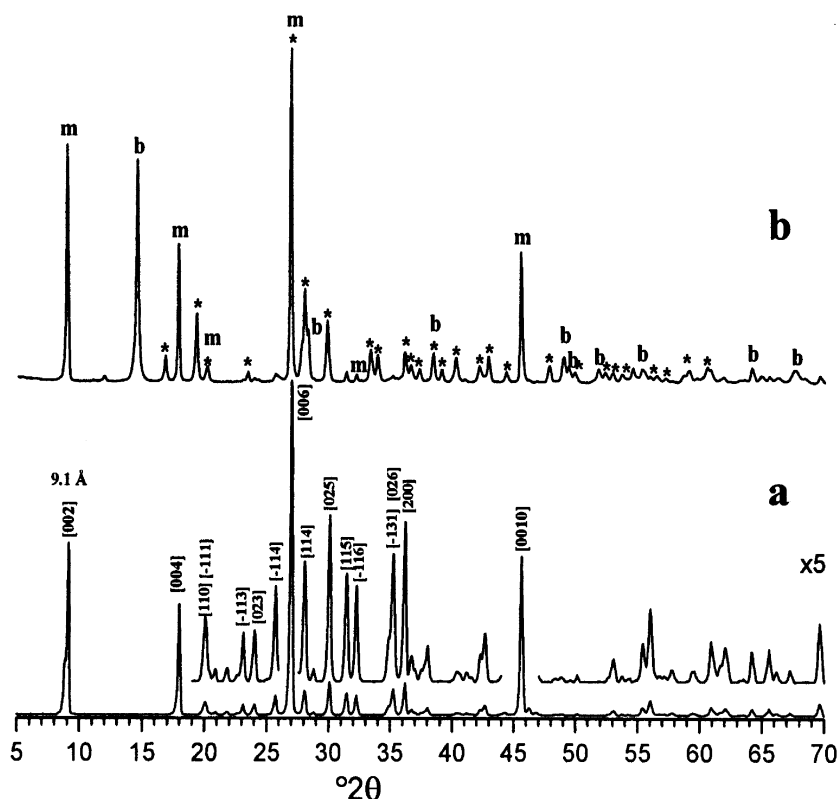


Figure 1. XRD patterns of muscovite: (a) untreated, and (b) hydrothermally treated with lutetium nitrate solution. m = muscovite (76-0668), b = boehmite (76-1871), \* = Lu<sub>2</sub>Si<sub>2</sub>O<sub>7</sub> (35-0326).

In order to provide direct information on the short-range changes that occur during the hydrothermal reaction, a study of the main constituents of the muscovite was carried out using MAS NMR spectroscopy. Figure 3a shows the <sup>29</sup>Si NMR spectra of the sample before (bottom) and after hydrothermal treatment (top). The <sup>29</sup>Si chemical shift of the untreated sample (−85.1 ppm) corresponds to Q<sup>3</sup>(1Al) environments and is in agreement with the values reported previously for muscovite (Lippmaa *et al.*, 1980). Sanz and Serratosa (1984a), using a low-Fe sample, resolved two weaker additional resonances at −89 and −81 ppm, which they assigned to Q<sup>3</sup>(0Al) and Q<sup>3</sup>(2Al) environments. However, Mackenzie *et al.* (1987) did not observe these two resonances and they explained this fact as either being due to peak broadening and poorer resolution because of the presence of paramagnetic Fe or because the tetrahedral Al was fully ordered within the tetrahedral structure. This situation has been shown by theoretical modeling (Herrero *et al.*, 1985) to give rise to a single Q<sup>3</sup>(1Al) resonance. Our spectrum agrees with that shown by Mackenzie *et al.* (1987) and a single broad signal at −85.1 ppm due to Q<sup>3</sup>(1Al) was observed.

Two signals at −91.7 and −84.4 ppm were observed in the <sup>29</sup>Si MAS NMR spectrum of the treated sample. The signal at a lower frequency has been assigned to the new phase Lu<sub>2</sub>Si<sub>2</sub>O<sub>7</sub> (Perdigón, 2002) and the one at a

higher frequency to the remnant muscovite. It is noticeable that the muscovite Si peak shifted to a lower field after the treatment. This indicates that, although the mica had not suffered any structural long-range order change, some structural short-range changes did occur. It has been reported (Alba *et al.*, 2001) that octahedral cations diffuse into the interlayer space during hydrothermal treatment, so that the octahedral vacancies increase during the treatment. In agreement with Weiss *et al.* (1987) a deshielding of Si was observed as octahedral occupancy decreases. Finally, from the integrated intensity of the peaks, 36.6% of total Si was estimated to be in the Lu<sub>2</sub>Si<sub>2</sub>O<sub>7</sub> phase.

Figure 3b shows the <sup>27</sup>Al MAS NMR spectra of the untreated (lower) and hydrothermally treated (upper) muscovite. Both spectra contain two resonances, at ~5 and 71 ppm, corresponding to Al in the octahedral and tetrahedral sites, respectively (Sanz and Serratosa, 1984b). A considerable decrease in the intensity of tetrahedral Al was observed after treatment due to the formation of new phases containing octahedral Al, such as boehmite.

#### Beidellite

Figure 4 shows the XRD patterns of beidellite before and after the hydrothermal treatment. In general, the XRD patterns corresponding to a dioctahedral smectite are made up of two distinct types of reflections, basal

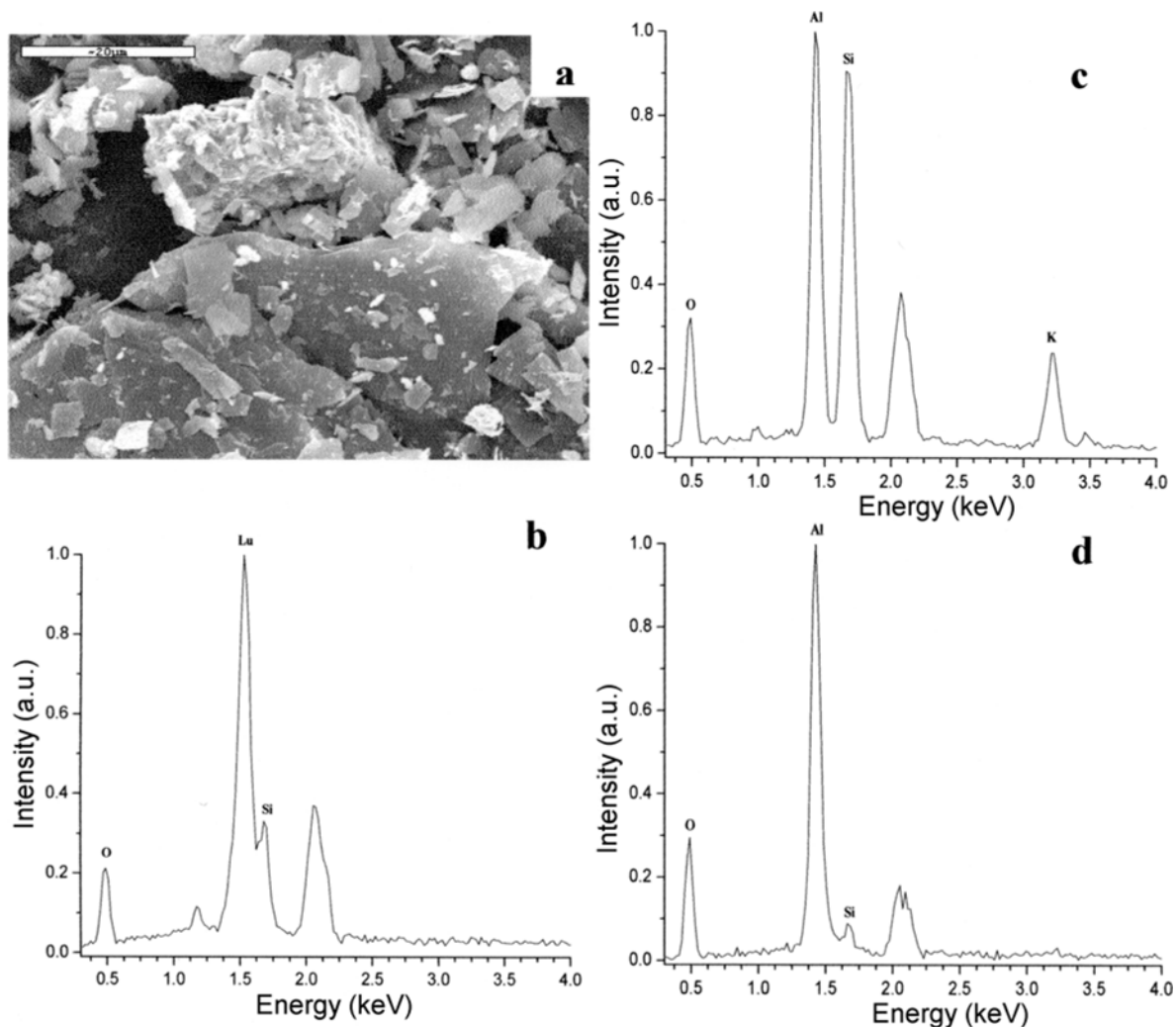


Figure 2. SEM image (a) and EDX spectra (b,c,d) of the hydrothermal reaction products of muscovite hydrothermally treated with lutetium nitrate solution.

and general, indexed in the patterns. The  $14.8 \text{ \AA}$   $d_{001}$  value of beidellite is compatible with a two-layer hydrate. The general reflections or  $hk$  bands are asymmetrical lines with a sharp peak and a long tailing-off. They are characteristic of the structure of the smectite layers themselves and independent of external conditions. Two reflections at  $7.1$  and  $3.5 \text{ \AA}$  have been assigned to the kaolinite impurity.

The XRD pattern of the beidellite submitted to hydrothermal treatment at  $300^\circ\text{C}$  for 3 days in  $\text{Lu}(\text{NO}_3)_3$  solution (Figure 4b) is considerably different from the previous pattern. It shows a set of well-resolved and narrow lines corresponding, mainly, to the crystallization of kaolinite (JCPDS chart 78-1996); additionally, reflections corresponding to  $\text{Lu}_2\text{Si}_2\text{O}_7$  (JCPDS chart 35-0326), boehmite (JCPDS chart 76-1871), and natrosilite,  $\beta\text{-Na}_2\text{Si}_2\text{O}_5$ , (JCPDS chart 23-0529) were observed. The absence of any reflection corresponding

to the smectite structure denotes the absence of a precursor in the reaction product. Thus, the reaction mechanism in this case probably involves the complete dissolution of smectite followed by the crystallization of new phases. This mechanism has already been observed in some smectite reaction processes such as smectite illitization (Nadeau *et al.*, 1984; Inoue *et al.*, 1987; Yau *et al.*, 1987; Eberl and Środoń, 1988; Ylagan *et al.*, 2000).

The SEM image of the sample after the hydrothermal treatment at  $300^\circ\text{C}$  for 3 days (Figure 5a) shows particles with different shapes. The majority of the particles had a lamellar appearance and had an EDX spectrum (Figure 5b) with peaks that correspond to the  $K\alpha_1$  lines of Si and Al, due to kaolinite. The large particle with sharp edges had a chemical composition compatible with  $\text{Lu}_2\text{Si}_2\text{O}_7$  (Figure 5c). No isolated particles of the other minor phases were observed.

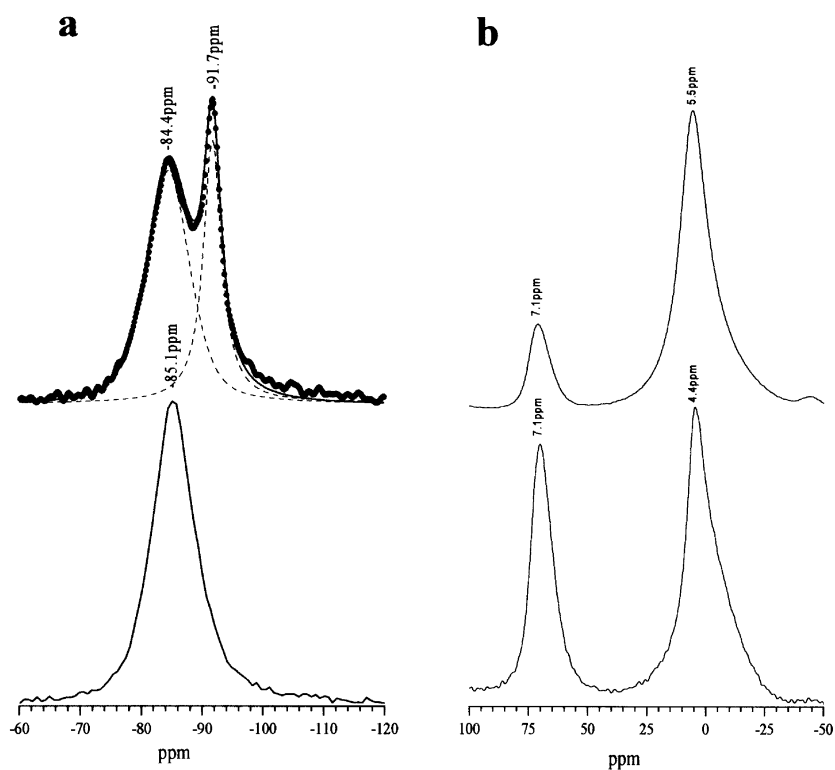


Figure 3. MAS NMR spectra of untreated (lower) and hydrothermally treated with lutetium nitrate solution (upper), muscovite: (a)  $^{29}\text{Si}$  MAS NMR spectra, and (b)  $^{27}\text{Al}$  MAS NMR spectra.

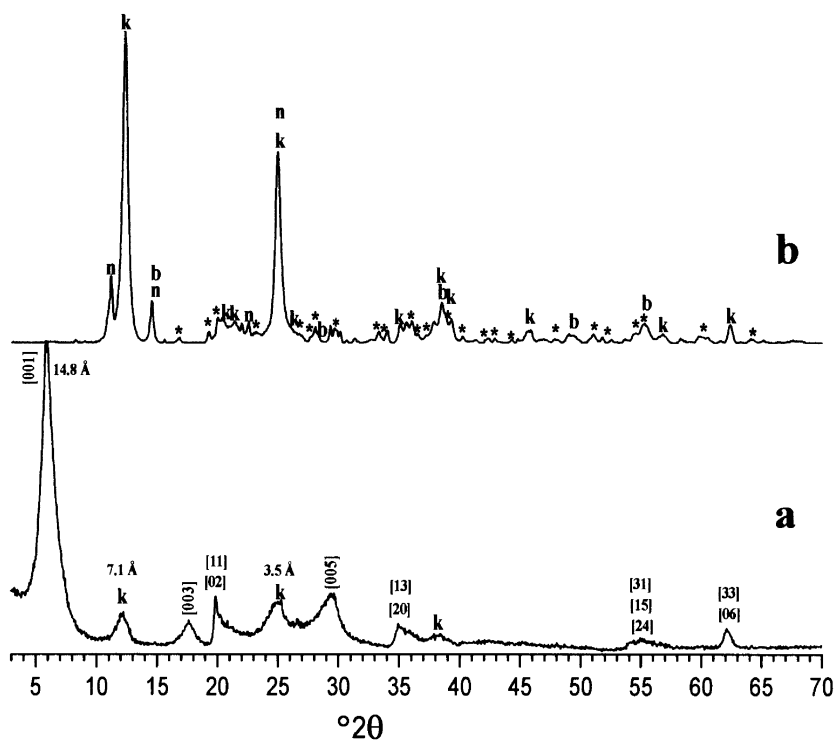


Figure 4. XRD patterns of beidellite: (a) untreated sample, and (b) hydrothermally treated with lutetium nitrate solution. k = kaolinite (78-1996), b = boehmite (76-1871), n = natrosilite (23-0529), \* =  $\text{Lu}_2\text{Si}_2\text{O}_7$  (35-0326).

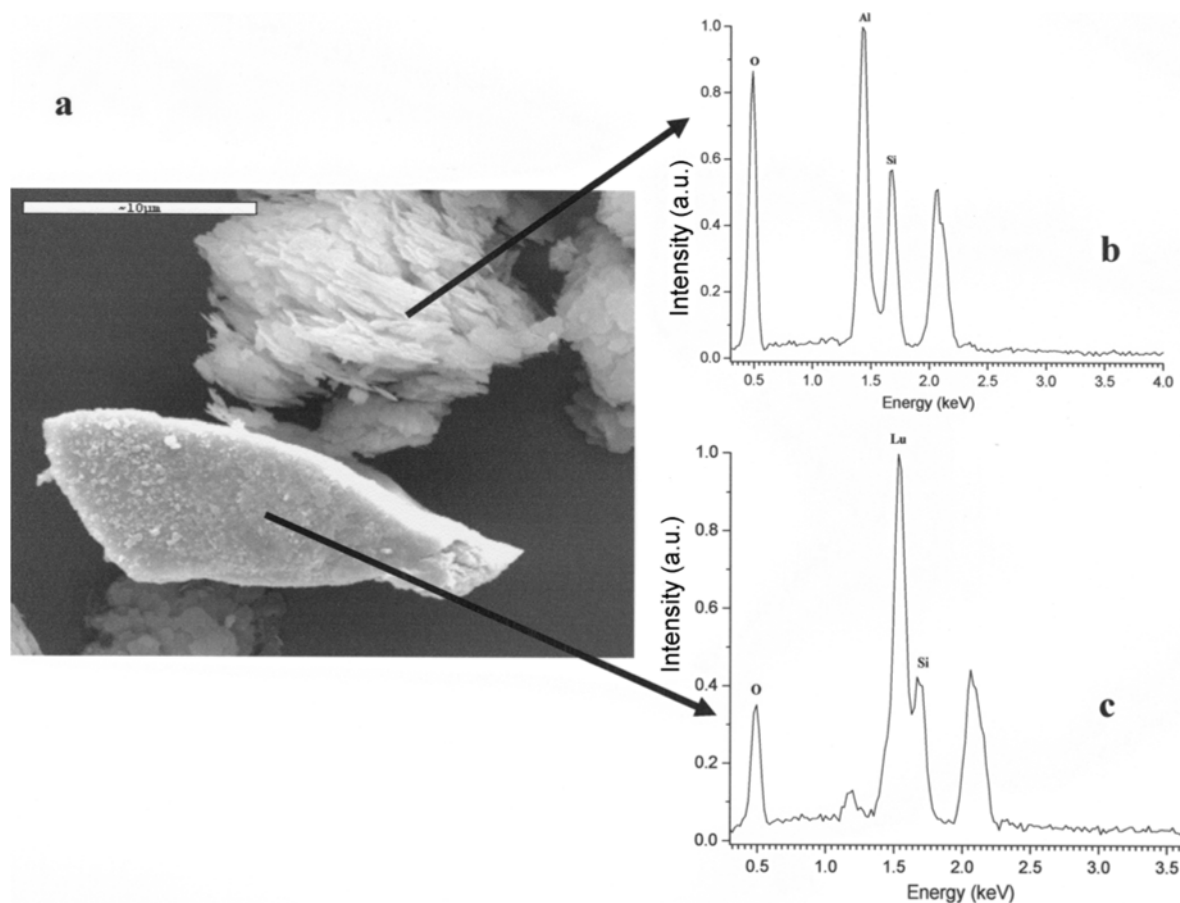


Figure 5. SEM image (a) and EDX spectra (b,c) of the hydrothermal reaction products of beidellite treated hydrothermally with lutetium nitrate solution.

Figure 6a shows the  $^{29}\text{Si}$  MAS NMR spectra of the untreated and hydrothermally treated beidellite. The  $^{29}\text{Si}$  spectrum of the untreated sample was in good agreement with that expected for beidellite (Becerro, 1997). The major component at  $-91.9$  ppm corresponds to  $\text{Q}^3(\text{OAl})$ ; it was accompanied by two minor contributions at  $-87.3$  and  $-83.2$  ppm due to  $\text{Q}^3(\text{1Al})$  and  $\text{Q}^3(\text{2Al})$ , respectively. The integrated intensities of these contributions, 80.9:16.0:0.8, are in good agreement with the Si/Al ratio, 17.1, shown in the formula. Additionally, a contribution at  $-91.2$  ppm due to the 2.3% Si in kaolinite was observed (Mackenzie and Smith, 2002). After hydrothermal treatment, three different  $^{29}\text{Si}$  environments were observed as being due to kaolinite ( $-91.2$  ppm), natrosilite ( $-87.5$  ppm) (Martaza, 1989) and  $\text{Lu}_2\text{Si}_2\text{O}_7$  ( $-91.7$  ppm) with integrated areas of 80.8%, 5.2% and 14.0%, respectively. No  $^{29}\text{Si}$  due to the original smectite was observed.

Figure 6b shows the  $^{27}\text{Al}$  MAS NMR spectra of the untreated and hydrothermally treated beidellite. The spectrum obtained for the untreated sample consists of two components centered at  $\sim 3$  and  $69$  ppm, corresponding to Al in octahedral and tetrahedral coordinations,

respectively (Sanz and Serratos, 1984b). This spectrum displays a drastic decrease in  $^{IV}\text{Al}$  that can be explained in terms of diffusion from its initial locations to form the new Al-containing crystalline phases, kaolinite and boehmite, where the Al is in octahedral coordination.

All these results indicate that Lu cations react with the silicon framework of both 2:1 layered aluminosilicates under hydrothermal conditions. Thus, the chemical mechanism of rare earth immobilization might well be efficient independent of the natural ageing of 2:1 layered aluminosilicates, which has been of concern in the use of bentonite as a buffer material in a nuclear waste repository.

However, the two materials behaved differently. On one hand, the extension of disilicate formation, evaluated by  $^{29}\text{Si}$  MAS NMR, depends on the nature of the aluminosilicate. The  $^{29}\text{Si}$  spectra revealed that 36.6% of Si belonged to  $\text{Lu}_2\text{Si}_2\text{O}_7$  in the treated muscovite vs. 14% in the treated beidellite. Also, the stability of the starting materials during the hydrothermal treatment was clearly different. The XRD patterns showed that the muscovite structure remained during the treatment while the beidellite structure was completely destroyed.

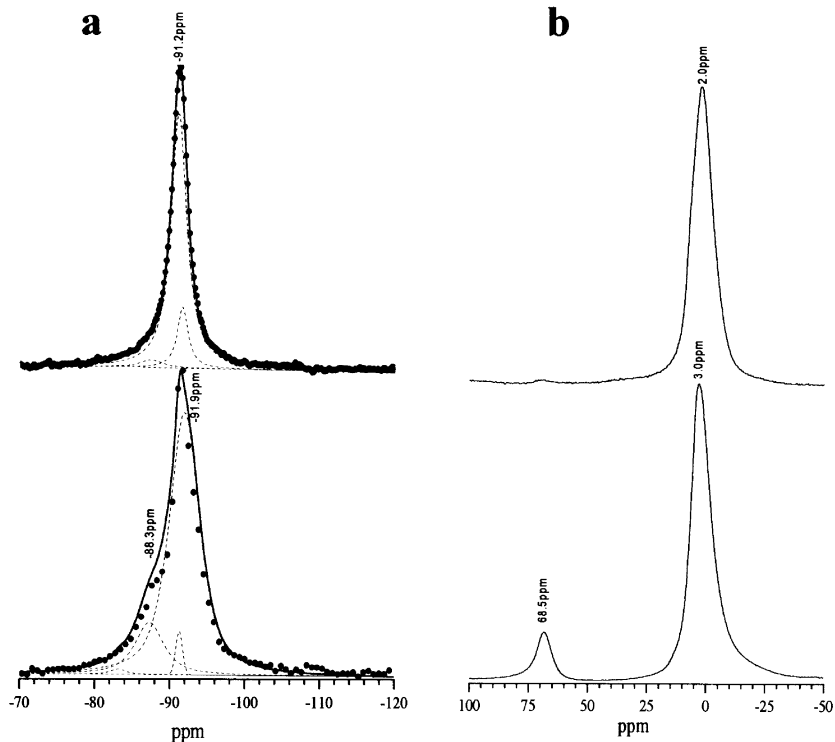


Figure 6. MAS NMR spectra of untreated (lower) and hydrothermally treated with lutetium nitrate solution (upper) beidellite: (a) experimental (dots), simulated (solid line), and contributions (dashed line) to the  $^{29}\text{Si}$  MAS NMR spectra, and (b)  $^{27}\text{Al}$  MAS NMR spectra.

## CONCLUSIONS

The swelling and CEC properties do not seem to be the characteristics of silicates that determine the reactivity. However, the stability of the silicate is important. If the silicate is not stable enough, complete dissolution of the silicate followed by crystallization of new phases would occur and the extent of reaction would be decreased. Thus, this study has made it clear that it is important to account for the chemical transformation that 2:1 layered silicates undergo during radionuclide disilicate formation. This is different from the effects observed with natural ageing, because it can affect the immobilization capacity of this material throughout subsequent radionuclide leaks.

## ACKNOWLEDGMENTS

We gratefully acknowledge M.C. Jiménez de Haro for her help with SEM, E. Jiménez Roca for the design and construction of the hydrothermal reactors, and financial support from the DGICYT (Projects no. BQU2001-3138 and MAT2002-03504).

## REFERENCES

- Alba, M.D., Becerro, A.I., Castro, M.A. and Perdígón, A.C. (2001) Hydrothermal reactivity of Lu-saturated smectites: Part I. A long-range order study. *American Mineralogist*, **86**, 115–123
- Allen, C.C. and Wood, M.I. (1988) Bentonite in Nuclear Waste Disposal: A Review of Research in Support of the Basalt Waste Isolation Project. *Applied Clay Science*, **3**, 11–30
- Ames, L.L., McGarrah, J.E., Walker, B.A. and Salter, P.F. (1982) Sorption of uranium and cesium by Hanford basalts and associated secondary smectite. *Chemical Geology*, **35**, 205–225.
- Ames, L.L., McGarrah, J.E. and Walker, B.A. (1983) Sorption of trace constituents from aqueous-solutions onto secondary minerals. 1. Uranium. *Clays and Clay Minerals*, **31**, 321–324.
- Bailey, S.W. (1980) Structures of layer silicates. Pp. 1–123 in: *Crystal Structures of Clay Minerals and their X-ray Identification* (G.W. Brindley, and G. Brown, editors). Mineralogical Society, London.
- Bauer, A., Schäfer, T., Dohrmann, R., Hoffmann, H. and Kim, J.J. (2001) Smectite stability in acid salt solutions and the fate of Eu, Th and U in solution. *Clay Minerals*, **36**, 93–103
- Becerro, A.I. (1997) Desarrollo de un sistema modelo de análisis estructural de la reactividad química de compuestos de silicio 2D y 3D aplicado a la formación de  $\text{Lu}_2\text{Si}_2\text{O}_7$ . PhD thesis, University of Seville, Spain.
- Borovec, Z. (1981) The adsorption of uranyl species by fine clays. *Chemical Geology*, **32**, 45–58.
- Chisholm-Brause, C., Conradson, S.D., Buscher, C.T., Eller, P.G. and Morris, D.E. (1994) Speciation of uranyl sorbed at multiple binding-sites on montmorillonite. *Geochimica et Cosmochimica Acta*, **58**, 3625.
- Cuadros, J. and Linares, J. (1996) Experimental kinetic study of the smectite-illite transformation. *Geochimica et Cosmochimica Acta*, **60**, 439–453
- Dent, A.J., Ramsay, J.D. and Swanton, S.W. (1992) An EXAFS study of uranyl-ion in solution and sorbed onto silica and montmorillonite clay colloids. *Journal of Colloid and*

- Interface Science*, **150**, 45–60.
- Eberl, D.D. and Srodoň, J. (1988) Ostwald ripening and interparticle-diffraction effects for illite crystals. *American Mineralogist*, **73**, 1335–1345
- Eberl, D.D., Velde, B. and McCormick, T. (1993) Synthesis of illite-smectite from smectite at earth surface temperatures and high pH. *Clay Minerals*, **28**, 49–60.
- Heimann, R.B. (1993) Bronsted acidification observed during hydrothermal treatment of a calcium montmorillonite. *Clays and Clay Minerals*, **41**, 718–725.
- Herrero, C.P., Sanz, J. and Serratos, J.M. (1985) Si, Al distribution in micas – analysis by high-resolution Si-29 NMR-spectroscopy. *Journal of Physics C: Solid State Physics*, **18**, 13–22.
- Inoue, A., Kohyama, N., Kitagawa, R. and Watanabe, T. (1987) Chemical and morphological evidence for the conversion of smectite to illite. *Clays and Clay Minerals*, **35**, 111–120.
- Jennings, S. and Thompson, G.R. (1986) Diagenesis of Plio-Pleistocene sediments of the Colorado River Delta, southern California. *Journal of Sedimentary Petrology*, **56**, 89–98.
- Lippmaa, E., Magi, M., Samoson, A., Engelhardt, G. and Grimmer, A.R. (1980) Structural studies of silicates by solid-state high-resolution Si-29 NMR. *Journal of the American Chemical Society*, **102**, 4889–4893.
- Mackenzie, K.J.D. and Smith, M.E. (2002) *Multinuclear Solid-State NMR of Inorganic Materials*. Pergamon, Amsterdam, 215 pp.
- Mackenzie, K.J.D., Brown, I.W.M., Cardile, C.M. and Meinhold, R.H. (1987) The thermal reaction of muscovite studied by high-resolution solid-state 29-Si and 27-Al NMR. *Journal of Materials Science*, **22**, 2645–2654.
- Martaza, M.G. (1989) A nuclear magnetic resonance investigation of the structure of some alkali silicates glasses. PhD thesis, University of Warwick, UK.
- Mather, J.D., Chapman, N.A., Black, J.H. and Lintern, B.C. (1982) The geological disposal of high-level radioactive waste – a review of the Institute of Geological Sciences Research programme. *Nuclear Energy*, **21**, 167–173.
- Meunier, A., Velde, B. and Griffault, V. (1998) The reactivity of bentonites: a review. An application to clay barrier stability for nuclear waste storage. *Clay Minerals*, **33**, 187–196.
- Miller, S.E., Heath, G.R. and González, R.D. (1982) Effects of temperature on the sorption of lanthanides by montmorillonite. *Clays and Clay Minerals*, **30**, 111–122.
- Morris, D.E., Chisholm-Brause, C.J., Barr, M.E., Conradson, S.D. and Eller, P.G. (1994) Optical spectroscopic studies of the sorption of  $\text{UO}_2^{2+}$  species on a reference smectite. *Geochimica et Cosmochimica Acta*, **58**, 3613–3623.
- Nadeau, P.H., Wilson, M.J., McHardy, W.J. and Tait, J.M. (1984) Interstratified clays as fundamental particles. *Science*, **225**, 923–925.
- Oades, J.M. (1984) Interactions of polycations of aluminum and iron with clays. *Clays and Clay Minerals*, **32**, 49–57.
- Perdigón, A.C. (2002) Estudio del sistema saponita/ $\text{Lu}(\text{NO}_3)_3/\text{H}_2\text{O}$  en condiciones hidrotérmicas. PhD thesis, University of Seville, Spain.
- Pérez-Maqueda, L.A., Franco, F., Avilés, M.A., Poyato, J. and Pérez-Rodríguez, J.L. (2003) Effect of sonication on particle-size distribution in natural muscovite and biotite. *Clays and Clay Minerals*, **51**, 701–708.
- Sanz, J. and Serratos, J.M. (1984a) Si-29 and Al-27 high-resolution MAS-NMR spectra of phyllosilicates. *Journal of the American Chemical Society*, **106**, 4790–4793.
- Sanz, J. and Serratos, J.M. (1984b) Distinction of tetrahedrally and octahedrally coordinated Al in phyllosilicates by NMR-spectroscopy. *Clay Minerals*, **19**, 113–115.
- Savage, D. and Chapman, N.A. (1982) Hydrothermal behaviour of simulated waste glass- and waste-rock interaction under repository conditions. *Chemical Geology*, **36**, 59–86.
- Tsunashima, A., Brindley, G.W. and Bastovanov, M. (1981) Adsorption of uranium from solutions by montmorillonite-compositions and properties of uranyl montmorillonites. *Clays and Clay Minerals*, **29**, 10–16.
- Weiss, C.A. Jr., Altaner, S.P. and Kirkpatrick, R.J. (1987) High-resolution  $^{29}\text{Si}$  NMR spectroscopy of 2:1 layer silicates: Correlations among chemical shift, structural distortions, and chemical variations. *American Mineralogist*, **72**, 935–942.
- Yamada, H. and Nakazawa, H. (1993) Isothermal treatments of regularly interstratified montmorillonite-beidellite at hydrothermal conditions. *Clays and Clay Minerals*, **41**, 726–730.
- Yau, Y.C., Peacor, D.R. and McDowell, S.D. (1987) Smectite-to-illite reactions in Salton Sea shales: A transmission and analytical electron microscopy study. *Journal of Sedimentary Petrology*, **57**, 335–342.
- Ylagan, R.F., Altaner, S.P. and Pozzuoli, A. (2000) Reaction mechanisms of smectite illitization associated with hydrothermal alteration from Ponza Island, Italy. *Clays and Clay Minerals*, **48**, 610–631.

(Received 7 May 2004; revised 10 August 2004; Ms. 914; A.E. William F. Jaynes)